World Academy of Science, Engineering and Technology
International Journal of Computer and Information Engineering
Vol:11, No:4, 2017

A Neuro-Automata Decision Support System for the Control of Late Blight in Tomato Crops

Gizelle K. Vianna, Gustavo S. Oliveira, Gabriel V. Cunha

***Abstract*—**The use of decision support systems in agriculture may help monitoring large fields of crops by automatically detecting the symptoms of foliage diseases. In our work, we designed and implemented a decision support system for small tomatoes producers. This work investigates ways to recognize the late blight disease from the analysis of digital images of tomatoes, using a pair of multilayer perceptron neural networks. The networks outputs are used to generate repainted tomato images in which the injuries on the plant are highlighted, and to calculate the damage level of each plant. Those levels are then used to construct a situation map of a farm where a cellular automata simulates the outbreak evolution over the fields. The simulator can test different pesticides actions, helping in the decision on when to start the spraying and in the analysis of losses and gains of each choice of action.

***Keywords*—**Artificial neural networks, cellular automata, decision support system, pattern recognition.

I. Introduction

IN Brazil, an important part of the economy depends on agriculture. In 2015, the agribusiness corresponded to 21.46% of Brazilian GDP, or more than US$400.00 million [1], [2]. Particularly, the tomato (*Solanum lycopersicon*) crop occupies seventh position in the rank of food plant tons produced per year, with more than 1.9 tons produced in 2014 [1], [3]. However, that plant is vulnerable to many diseases and it ranks the second position in pesticide consumption per planted area in Brazil [4], thus it is essential that farmers maintain a strict control over the quality of their crops. On the other hand, tomatoes are typically produced in small farms and require continuous monitoring from experts, which might be prohibitively expensive and time-consuming.

The most common disease that affects tomato crops worldwide is the late blight, caused by *Phytophthora infestans*, a fungus that inhabits the soil and disseminates through spores. Farmers and workers visually recognize the disease by the appearance of dark brown lesions on tomato leaves that vary from brown or gray to pale green, often situated at the edges of the leaves. The disease first appears as water-soaked areas that enlarge rapidly, developing into large brown necrotic areas, causing loss of leaves and, in severe cases, the plant death [5]-[7]. The disease occurs especially in cold and humid months when the dispersion of spores is facilitated by wind and high humidity. The disease can spread quickly under favorable climatic conditions consisting of a combination of relative humidity under 90% and temperature around 20°C (68°F). As a result, we have an epidemic that can lead to considerable losses in production [5], [8], and [9].

After analyzing some samples of plants from the farm, the farmers estimate the mean infestation degree at the area and define a schedule of pesticide spraying. Unfortunately, we are facing the emergence of resistant fungus variants, and a second generation of fungicides began to be used, so it is critical to use fungicides in proper doses and intervals [10]-[13]. According to [9], [14]-[16], with the aid of information technology for early detection of crop diseases, it is possible to delay the beginning of pesticides spraying to obtain an average reduction of 50% in total sprays, reaching rates of 80% reduction in some cases.

The goal of this paper is to present a computer-based solution that may help farmers to make better decisions to combat late blight on tomato crops, expanding previous works [17]-[19]. This research aims at helping the detection of late blight in tomato crops, and the measuring of the damage level at each plant, by using a pattern recognition system based on multilayer perceptron neural networks (MLP). We also developed a decision support system that generates simulations of spreading scenarios of contamination and tests alternatives for combating the disease, supported by meteorological data and well-known prediction models of the late blight.

II. Pattern Recognition in Diagnosis of Tomato Diseases

Image processing is a useful tool for analysis in various agricultural applications and several studies have also investigated the use of broadband color, or chromaticity values, for plant species recognition [14], [20]-[23]. In this paper, we used the color tones from individual pixels of the leaves to classify them in one of the seven possible degrees of the scale defined by [6]. We also used a mean filter to reduce the details of abrupt color changes, which improved the performance of our pattern classifier.

At the beginning of this research, we have decided to provide our target users the free use of our classification system, as soon as it would be in production. In addition, as they are small farmers, they may not afford expensive equipment or might be unable to operate it properly. Thus, we have not used any sophisticated machinery or proprietary software packages in order to lower the cost of the final

G. K. Vianna is with the Universidade Federal Rural do Rio de Janeiro, Seropedica, CEP Brazil (corresponding author, phone: 55-21-2682-1469, e-mail: kupac@ufrrj.br).

G. V. Cunha and G. S. Oliveira are with the Universidade Federal Rural do Rio de Janeiro, Seropedica, CEP Brazil (e-mails: gabrielvcunha@gmail.com, gustaves2519@yahoo.com.br).

We would like to thank FAPERJ (Edital APQ1/2015, Processo nº 210.704/2016) for partial financial support.

system. Based on that premise, we have worked upon digital images obtained by low-resolution built-in cell phone cameras. The pictures were taken in an open environment under natural sunlight conditions. The tomato plants were cultivated in the experimental fields of the Horticulture Department of our institution in a cropping area historically linked with the natural occurrence of late blight. Besides, the images may have some noise like soil, fruits, parts of the sky and the earth.

We used a combination of two artificial neural networks (ANN) to perform, for each pixel, its classification into one of three possible categories: healthy, injured or background. The combination of the results of two ANN's would provide the final classification of each pixel. After classifying all the pixels of one single image, we used the class information of all these pixels to compute the final classification of the whole leaf, assigning it a degree of contamination, as defined in [6].

For each image, we generated a text file containing, for each pixel, the X-Y coordinates of the pixel and its RGB and HSL values. Next, all variables were linearly normalized, generating a new data table containing RGB and HSL values, varying from 0 to 1, which suits better to the training process of an ANN. We chose that normalization technique because the variable scales are similar (R, G, and B varies from 0 to 255; H vary from 0 to 359; S and L varies from 0 to 100) and because, as the domain is limited, there is no possibility of occurring outliers.

A. Pattern Recognition System

We conducted an experiment using two different ANNs. The first ANN was trained to recognize the green tones of the leaf or, in other words, healthy pixels. If a pixel was recognized as healthy, the ANN answer would be 1 (class 1), but if it was considered as belonging to the non-healthy class, the ANN answer should be 0 (class 0). The training of the latter ANN was similar, but it was conducted to recognize brown tones of the leaf, or injured pixels. For the ANN's training, we fist chose some pixels from specific areas of our available pre-processed images. As each image can give us around 1,500 pixels, we have used no more than four images to construct the training subset for the ANN's, where each record contained the color information plus the class label. The classification of each pixel considers the values of their R, G and B components from the RGB color system plus H, S, and L components from the HSL color system. We selected over 6,000 different labeled pixels, where around 2,000 came from each class. The classes could be green (corresponding to the different green tones a healthy leaf could have), red (the different brown tones a leaf affected by late blight could have), or background (which includes earth, sky, sticks and other noise colors). Examples of healthy pixels, injured pixels and backgrounds are shown in Fig. 1.

After labeling each pixel according to their classes, the three datasets were joined, shuffled, and linearly normalized, as explained above. We divided the resulting dataset in a 5:2 proportion, and then circa 5,000 records were used for the pair of ANN's training and around 2,000 for testing them.

(a) (b) (c)

Fig. 1 Each image shows one subset of pixels used to train the pair of ANN´s. Each subset corresponds to one different class and was built by pixels extracted from digital images of tomato leaves (a) Green: pixels from healthy areas of the leaves, (b) Red: pixels from injured areas and (c) background pixels

We have evaluated many ANN configurations, varying the learning rate from 0.4 up to 0.8 (with steps of 0.2), the momentum from 0.5 up to 0.9 (with steps of 0.2), and the number of hidden neurons from 4 up to 20, for one or two hidden layers of neurons. We have also tested different activation functions (such as hyperbolic tangent, sigmoid and purelin) in different combinations through the neuron layers.

Each different configuration was trained and tested 20 times in order to find the best one on average, in a total of 1,728 different ANN models. For each training, 1,200 records were randomly chosen from our labeled training dataset. Similarly, for each test, we randomly selected 500 labeled records from the testing dataset.

Finally, we chose the configuration with the best performance for each ANN. For the *green*-ANN, the best configuration was the 16-8-1 network, with training rate equal to 0.8, *momentum* equal to 0.9, and sigmoid activation function at all levels and a value of 0.5 for the threshold between the outputs. After analyzing each network from the total amount of 20 networks trained and tested with this configuration, we chose to use the one that achieved the best accuracy rate, which was a rate of about 97.99% in correct pixel classification. For the *red*-ANN, the best configuration was the 16-16-1 network, with training rate equal to 0.6, *momentum* equal to 0.7, and sigmoid activation function at all levels and the same value of 0.5 for the threshold. For that configuration, we chose the one with a rate of about 97.92% in correct pixel classification.

III. The Neural Network Classifier

After the training phase, we tested the ANN system with 60 new different leaf images. First, each image was pre-processed, having its definition reduced and being mean-filtered, as explained above. Second, for each image, we extracted the x and y coordinates and the RGB and HSL values of each pixel, and that information was stored in a different file for each image. Last, each record of a file was classified by the pair of ANN's and this final classification of each pixel from one single image was used to reconstruct the leaf image, and converted into a three-colored codification, where the new image contains only green, red or black pixels. During the conversion processes, we also calculated the ratio of red pixels over green pixels for each image. Finally, that ratio was then used to define the degree of late blight infestation of each leaf.

The detailed algorithm, from the original digital image until the definition of infestation degree of a single leaf, is conducted as follows:

1) A JPEG image of a leaf, took in the open field, has its definition reduced, is mean-filtered and processed into a text file that contains, for each pixel, its *x* and *y* coordinates, RGB values, and HSL values.
2) Each line of the text file generated in step 1 was converted into a register in a CSV spreadsheet. Each column, or variable, from the spreadsheet is linearly normalized.
3) Each record from the CSV file is presented to both ANNs, already trained, and a new text file is built. That last file contains, for each pixel, only its x and y coordinates, and its final class, assigned from the combination of answers of the two ANNs, as follows:

3.1) The responses of each ANN are rounded to zero or one.
3.2) If the *green*-ANN response is greater than the *red*-ANN response, which corresponds to an answer equal to 1 for the *green*-ANN and 0 for the *red*-ANN, the pixel will be classified as *healthy*, and will be converted into just green, or RGB=(0,255,0).
3.3) If the *red*-ANN response is greater than the *green*-ANN response, which corresponds to an answer equal to 1 for the *red*-ANN and 0 for the *green*-ANN, the pixel will be classified as *injured*, and will be converted into just red, or RGB=(255,0,0).
3.4) If the *red*-ANN and *green*-ANN answers are equal, which corresponds to both answers being equal to 1 or equal to 0, the pixel will be classified as *background* and will be turned to black, or RGB=(0,0,0).

The text file constructed for each image in step 3 was used to reconstruct the JPEG image, and to calculate the injured level, based on [6], of the whole image, as shown in (1):

$$injured\ level = \frac{number\ of\ injured\ pixels}{total\ number\ of\ leaf\ pixels} \times 100 \quad (1)$$

In (1), the *total number of leaf pixels* accounts only for pixels belonging to the leaf itself (healthy plus injured), despising all background pixels, whereas the *injured level* indicates the percentage of injured areas over one leaf. We did not count black pixels, as they were not relevant to the final goal, which is to discover the damage extension of the leaf. The injured level was then used to assign, for each image, a status number, as shown in Table I. That status represents the health condition of the corresponding tomato plant and Fig. 2 shows some examples of original images and their respective codified images.

TABLE I
STATUS FOR EACH RANGE OF DAMAGE PERCENTAGE, BASED ON [6]

Status	0	1	2	3	4	5	6
% of damage	= 0	0-3	3-12	12-22	22-40	40-76	>=77

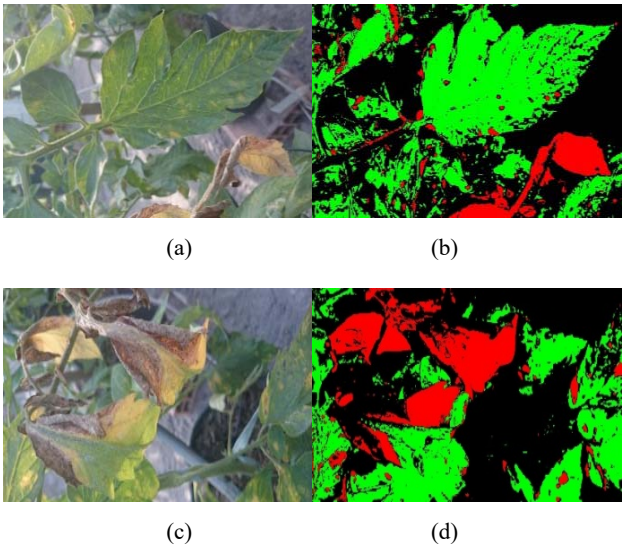

(a) (b) (c) (d)

Fig. 2 Examples of injured leafs from tomatoes, taken in our experimental field, infected by P. infestans. The images illustrate the images before and after the classification process. (a) was accounted as having a 15% of damage, or status 2, whereas (d) was accounted for 32%, or status 4. It is important to notice that the account was made considering the whole group of leave captured by the camera, which was considered to belong to the same plant

IV. THE DECISION SUPPORT SYSTEM

According to the Integrated Pest Management Program of California University [24], there are several reputable prediction models of late blight propagation in tomato and potato crops. Among those, we have chosen the Hyre's prediction model [25] that indicates that an initial outbreak of late blight will occur between seven to 14 days after 10 consecutive favorable days. A favorable day, in turn, occurs after five consecutive days where the mean temperature stays between 7.0°C and 25.5°C (48°F and 78°F) and, at the same time, after 10 days with a total precipitation equal to, or higher than, 30 millimeters (1.2 inches).

A. The Forecasting Model

A forecasting model should perform multi-day simulations and, for that reason, we needed to use more than 10 days of meteorological prediction and from very specific regions. To solve that requirement, we have used historical data, obtained through the National Institute of Meteorology [26], to calculate the mean of some meteorological variables in specific periods of the year, chosen by the system user during the simulation. We tested the system using the data from the city of Paty do Alferes, one of the main tomato producing regions of Brazil. Thus, we collected meteorological data from that region from 01/01/1999 until 01/01/2015, which includes temperature, relative humidity, minimum temperature, maximum temperature and precipitation.

The system user can choose the size of the data window that will be used in the historical average calculation, which can be five, 10 or 15 years, for all available variables. Finally, those historical averages are used to estimate the meteorological

variables for each day of the period of simulation, as exemplified in Table II.

B. The Cellular Automata Model

We have used a cellular automata (CA) to model the dynamics of late blight, defined in the two-dimensional domain, with Moore's neighborhood and a probabilistic transition function. The CA works over a matrix that represents a cultivated area of tomatoes where each cell represents a tomato plant that has a health condition value, or status, associated with it (Fig. 3 (a)).

The user defines the variable CA parameter *wind direction* that controls the direction of the status changes. The status of any cell would only change if it can be reached by an infected cell in its neighborhood and if the wind direction allows this contact (Fig. 3 (b)).

TABLE II
EXAMPLE OF CALCULATION OF THE EXPECTED TEMPERATURE FOR JUNE 6TH, 2016, USING THE HISTORICAL AVERAGE TEMPERATURES AND A 5-YEARS WINDOW

Day to be Simulated	2010	2011	2012	2013	2014	Average Result
06/06/16	17.42	11.24	21.64	18.48	16,88	**17,13**

(a) (b)

Fig. 3 (a) CA matrix where each cell the plants of a farm. (b) Example of a cell, which has an infection status 3, affecting their neighbors according to the wind direction

TABLE III
RULES FOR CALCULATION OF WEIGHT P

		1	2	3	4	5	6
Qs> 1	**Qd> = 10**	0.1	0.8	1.4	1.6	1.8	2
	10> Qd> = 7	0.1	0.5	1	1.1	1.2	1.4
Qs> 3	**7> Qd> = 5**	0.2	0.4	0.6	0.7	0.8	0.9

$$E'\big(c(i,j)\big) = E(c(i,j) + \sum_{n=1}^{8} P\left(v_n\big(c(i,j)\big)\right) - C * E(c(i,j)) \qquad (2)$$

The next status of each cell *c(i,j)*, where *i* is the line and *j* is the column, depends on its current status, *E(c(i,j))*, and on the current status of all its neighbors, in a neighborhood of size 8. An infected cell could have its status worsened when there are infected cells in its neighbor, or improved, when a technique *C* for combating the disease is being used. Each neighbor can affect a cell *c(i,j)* in a weighted way, according to the factors indicated by Hyre's model. The weighted influence of each neighbor is calculated following the rules shown in Table III, which considered the number of outbreaks *Qo*, the number of favorable days *Qf*, and the current status *E* of cell *c(I, j)*. Each cell in a neighborhood would also change its value in the next step, and the combination of all changes would build the new status matrix.

We have tested two forms of combat and, according to the literature [27], the combat type 1, which uses Dimethimorph, could decrease the status of a cell by 30% of the current status. On the other hand, combat type 2, which uses Metalaxyl-M+Mancozeb, could decrease the status by 20%. Thus, when using a combat method, the CA dynamics can be summarized by Table III and (2).

V. RESULTS AND DISCUSSION

Our approach was to convert the original JPEG images into codified red/green images, which proved to be effective in highlighting the injuries of the leaves. On the other hand, the codification process was able to overcome problems such as low resolution, focus, and image blur of the digital images, with no need to use more sophisticated digital image algorithms (e.g. contour detection).

Since we have worked with images captured in the field, in natural sunlight and taken by cell phones cameras, it was expected that they would contain a large amount of noise. As future work, we will include more image filtering processes, aiming at noise removal or attenuation. We are currently working in a module that uses the low-pass Median Filtering, and some Background Subtraction techniques to improve the data quality, and the results will be presented soon.

The simulation system is capable of mapping the streets and lines of a farm, registering georeferenced images of infected tomatoes. It can simulate scenarios of contagion spreading in a determined period of days and is possible to stop the simulation at any time to choose a combat method for the disease and then resume the simulation. The system's main functions are the module for processing and classification of digital tomato images described in previous sections, and the simulator that generates scenarios of the spreading of contamination and alternatives to combat the disease.

In the module for processing and classification, the images are classified within the status scale. Thus, they are placed in a matrix based on their real georeferenced information and the cell is painted with a different color for each different status (Table IV). The resulting matrix thus conceptually represents a map of the cultivated area being monitored by the system (Fig. 4 (a)). In the map, it is possible to select any cell and retrieve the corresponding sample information, including the original leaf image, the current health condition of the plant and the location of the plant in the field (Fig. 4 (b)).

TABLE IV
CORRESPONDENCE OF MAP CELLS FOR EACH POSSIBLE STATUS

Status	**0**	**1**	**2**	**3**	**4**	**5**	**6**
Cell color	Dark green	Green	Light green	Yellow	Orange	Dark Orange	Reddish orange

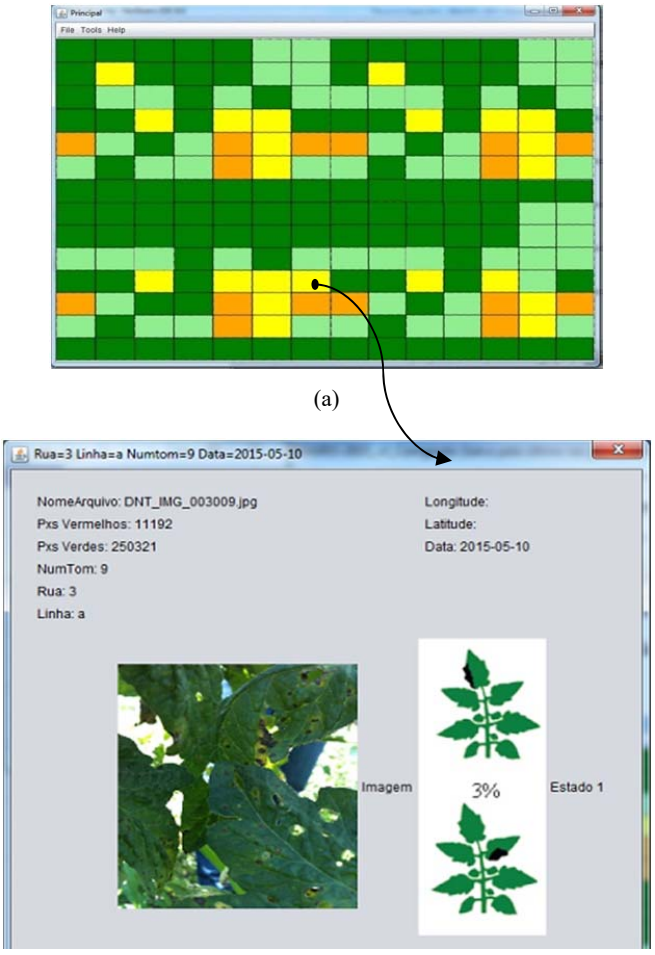

(a)

(b)

Fig. 4 (a) Conceptual map of a cultivated area of tomatoes from a monitored farm. (b) Details from a selected tomato on the map

In the simulation module, it is possible to run simulations of late blight spreading and visualize it in the conceptual map of the cultivated area (Fig. 5). It is also possible to analyze strategies to combat the disease. The simulation is interactive and simple, and the user can pause, resume or restart the simulation at any stage.

If a combat is tested during the simulation, a new dynamic could occur, reducing the status of tomatoes, depending on the contamination level of the field as a whole, the climatic factors, and the type of combat chosen. Fig. 6 shows what happens when combat type 2 is used on the 12th day of simulation. Starting from the same situation of Fig. 5 (a), it is possible to see that the losses could be minimized in the end of the 30th day of simulation.

We are already working on a panel of statistics that will show the performance of the simulation, displaying the financial results obtained by the chosen specific combat strategy, and comparing the costs of using the pesticides against not using any at all.

We have modeled the dynamics of two chemical fungicides to be available in this first version of our simulator because they are the most common in Brazil for tomato blight control. However, it is relatively simple to model new chemical control methods, and we are working on a tool that enables the user to do so.

We believe that this research is a suitable contribution to help small farmers in the early detection of late blight. The alternative we presented can accelerate the identification of the disease and help measuring the extension of the infestation. Plus, it can help small farmers to plan better the best time for spraying fungicides, protecting the environment while reducing the plantation costs.

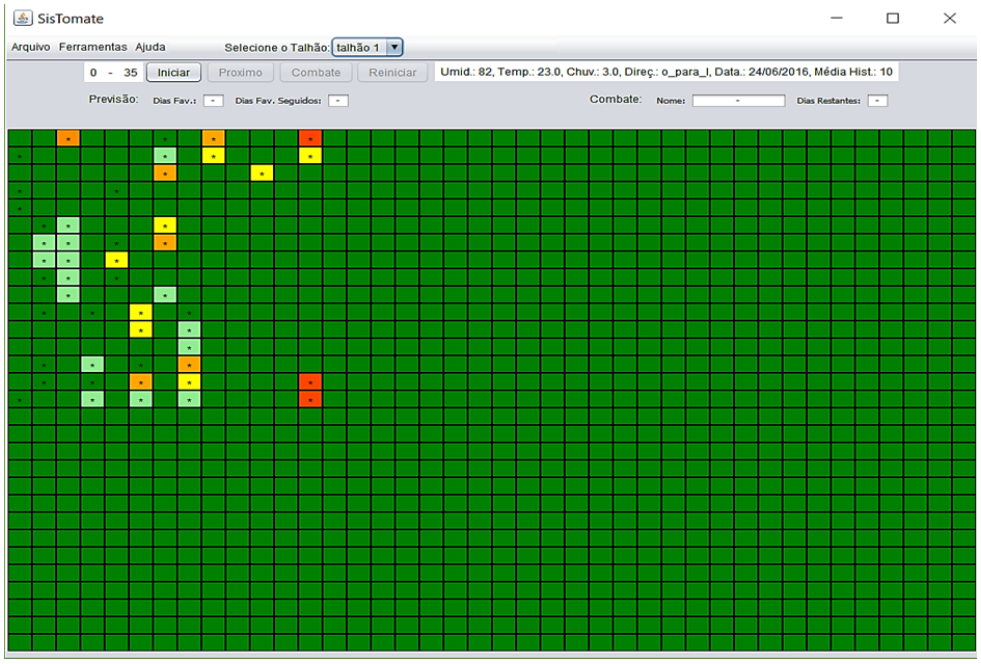

(a)

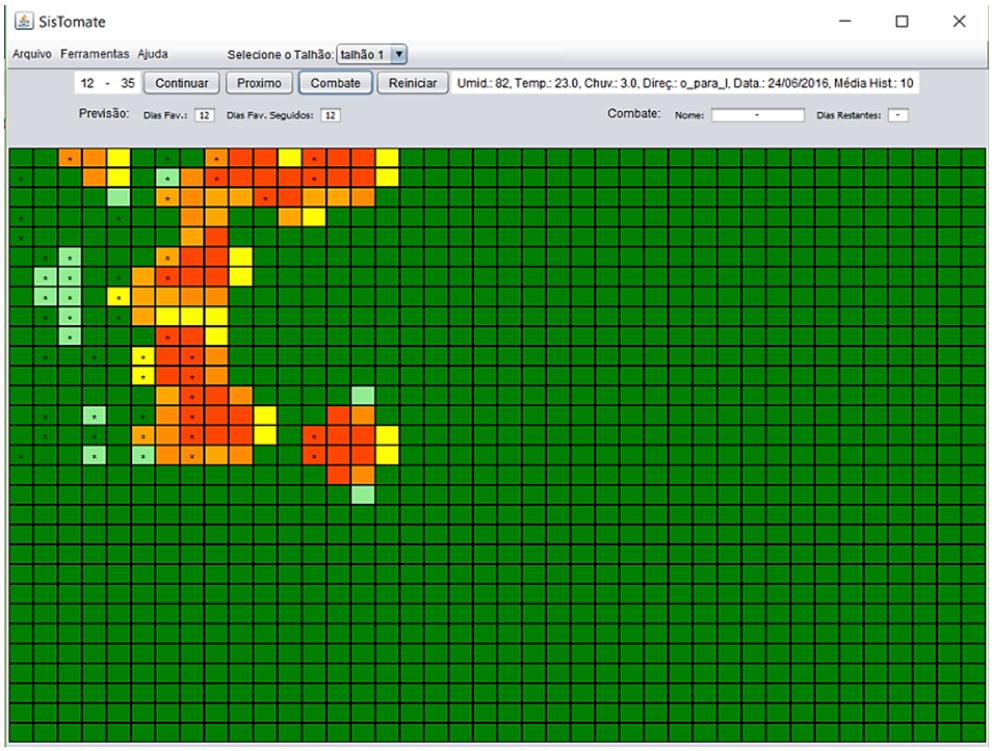

(b)

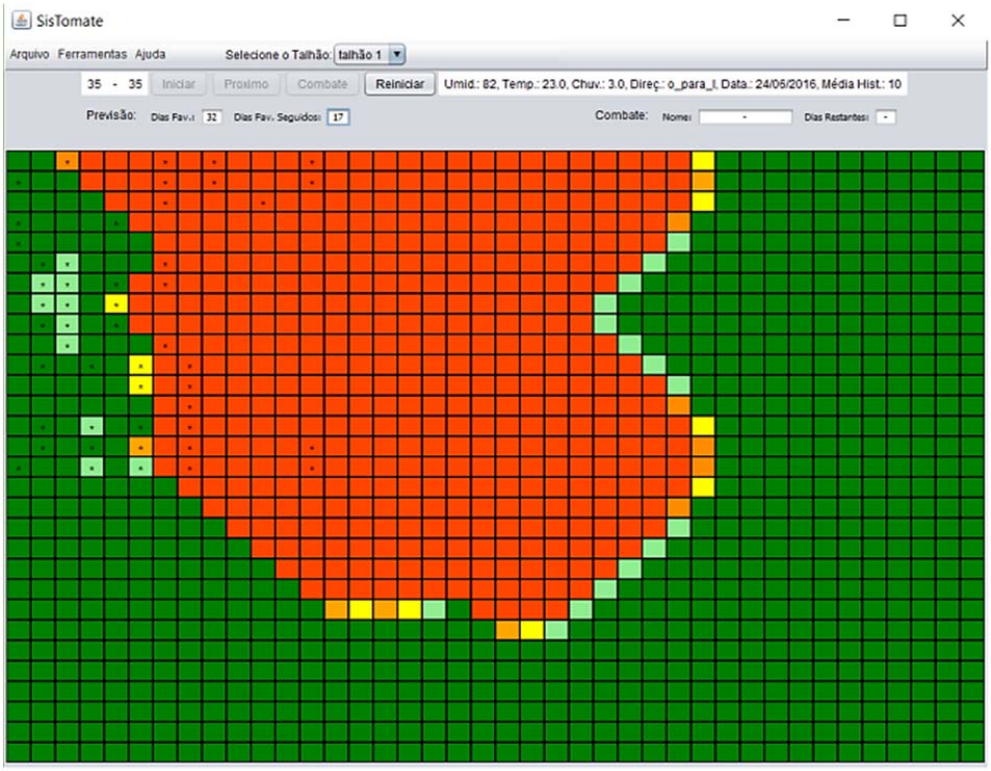

(c)

Fig. 5 A non-combat simulation starting at 06/24/2016, having wind direction from west to east and conducted during 35 iterations on a matrix with 1200 elements, where each cell represents one tomato plant. (a) At the beginning, before the simulation starts, with cells containing the original status of each plant, collected *in loco* (cells marked with an '*' represents one photographed plant, while the others have their status all settled to 0-healhy); (b) The map situation at iteration number 12, which means that the map represents the farm situation after 12 days from the initial day; (c) The map situation at the 35th day, when the simulation ends

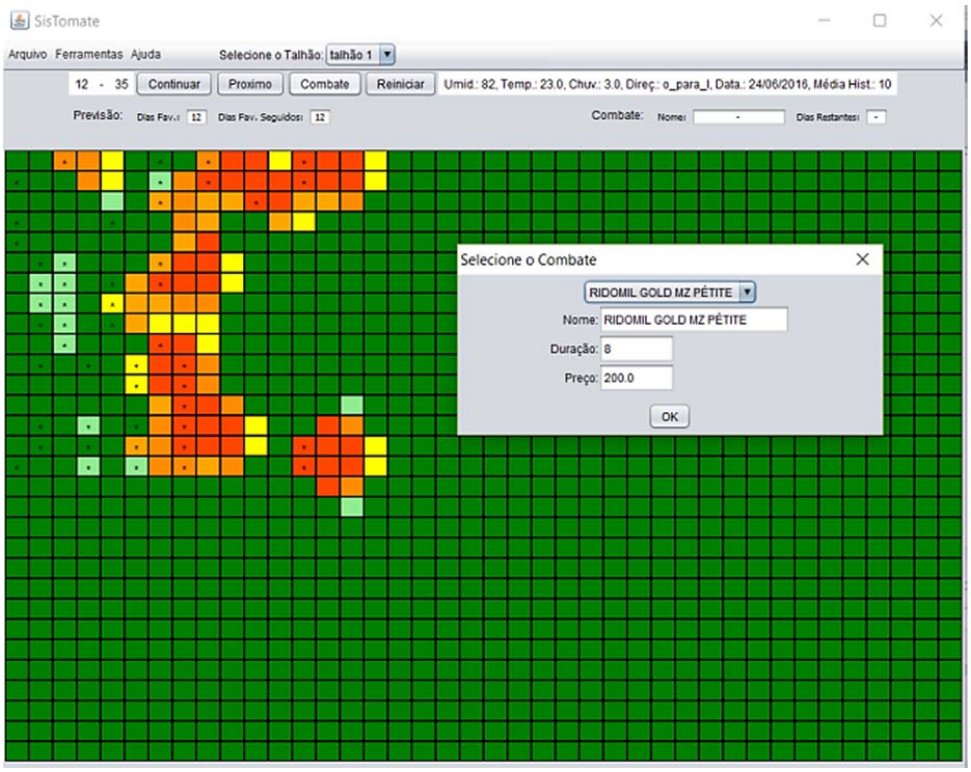

(a)

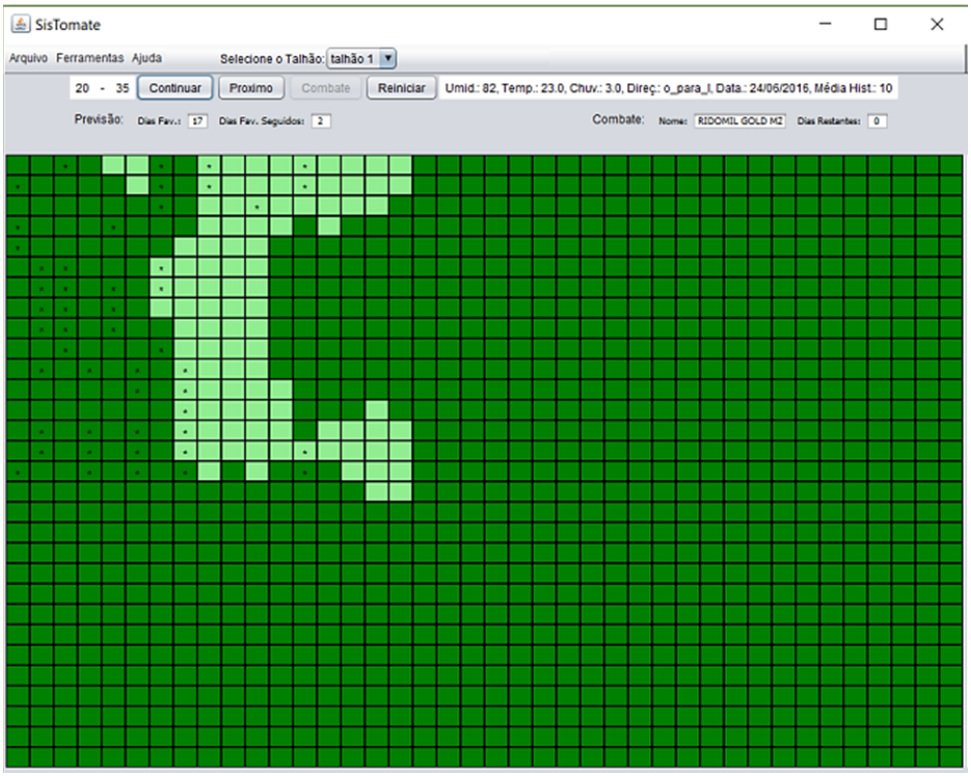

(b)

Fig. 6 A combat type 2 simulation starting at 06/24/2016, having wind direction from west to east and conducted during 35 iterations on a matrix with 1200 elements, where each cell represents one tomato plant. (a) On the 12th day of simulation, the combat type 2 was selected and the simulation was resumed; (b) The map situation at iteration number 35, when the simulation ends

REFERENCES

[1] IBGE (Instituto Brasileiro de Geografia e Estatística). *Sistema IBGE de Recuperação Automática - SIDRA*, Retrieved from http://www.sidra.ibge.gov.br/bda/agric/default.asp?z=t&o=11&i=P, in October 18, 2016.

[2] MAPA (Ministério da Agricultura Pecuária e Abastecimento), *Estatísticas e Dados Básicos de Economia Agrícola*, Retrieved from http://www.agricultura.gov.br/arq_editor/Pasta%20de%20Setembro%20-%202016.pdf, in October 10, 2016.

[3] M. Rabelo, "Faeg participa do Congresso Brasileiro de Tomate Industrial". Retrieved from: http://sistemafaeg.com.br/noticias/ 10796-faeg-participa-do-congresso-brasileiro-de-tomate-industrial, in May, 2015.

[4] E. M. Neves, L. Rodrigues, M. Dayoub, and D. S. Dragone, "Bataticultura: dispêndios com defensivos agrícolas no quinquênio 1997-2001,".*Batata Show*, vol. 6, pp. 22-23, 2003.

[5] USDA (United States Department of Agriculture), *USABlight Project*, Retrieved from https://usablight.org/node/29, in October 4, 2016.

[6] F.M. Correa, J.S.S. Bueno Filho, and M.G.F. Carmo, "Comparison of three diagrammatic keys for the quantification of late blight in tomato leaves," *Plant Pathology*, vol. 58, pp.:1128-1133,2009.

[7] J.R. Macedo, C.L. Capeche, A. Melo da S., and S.B. Bhering, "Recomendações Técnicas para a Produção do Tomate Ecologicamente Cultivado," *Manejo do Solo - Circular Técnica*, vol. 33. Rio de Janeiro: Embrapa Solos, 2005.

[8] E.S.G. Mizubuti, J.M.N. Maziero, L.A. Maffia, F. Haddad, and M.A Lima, "CGTE Program: Simulation, Epidemiology and Management of Late Blight," in *Global Initiative on Late Blight Conference*, Hamburg, Germany, 2002.

[9] W.F. Becker, "Validação de dois sistemas de previsão para o controle da requeima do tomateiro na região de Caçador, SC," *Agropecuária Catarinense*, vol.18, pp. 63-68, 2005.

[10] A. Saxena, B.K. Sarma, and H.B. Singh, "Effect of Azoxystrobin Based Fungicides in Management of Chilli and Tomato Diseases," *Proced. National Academy of Sciences*, India:Springer, 2014.

[11] C. Zhang, et al. "Fine mapping of the Ph-3 gene conferring resistance to late blight (Phytophthora infestans) in tomato," *Theor. Appl. Genet.*, vol. 126, Springer-Verlag, pp.:2643-2653, 2013.

[12] D.H. Park, Y. Zhang, and B.S. Kim, "Improvement of resistance to late blight in hybrid tomato," *Hort. Environm. Biotechnol*, vol. 55(2), Springer, pp.:120-124, 2014.

[13] O. Goufo, T. Mofor, and D. Ngnokam, "High Efficacy of Extracts of Cameroon Plants Against Tomato Late Blight Disease," *Agronomy for Sustainable Development*, vol. 8, INRA, EDP Sciences, pp.567-573, 2008.

[14] S. Sankaran, A. Mishraa, R. Ehsani, and C. Davis, "A review of advanced techniques for detecting plant diseases," *Computers and Electronics in Agriculture*, vol. 72, n.1, pp.:1-13, 2010.

[15] A.K. Mahlein, E.-C. Oerke, U. Steiner, and H.-W. Dehne, "Recent advances in sensing plant diseases for precision crop protection," *European Journal of Plant Pathology*, vol. 133, n.1, pp.:197-209, 2012.

[16] R. Bugiani, et al., "Monitoring airborne concentrations of sporangia of Phytophthora infestans in relation to tomato late blight in Emilia Romagna, Italy," *International Journal of Aerobiology*, vol. 11, pp.:41-46, Elsevier Science, 1995.

[17] G.K. Vianna and S.M.S. Cruz, "Análise inteligente de imagens digitais no monitoramento da requeima em tomateiros," *Anais do IX Congresso Brasileiro de Agroinformática*. Cuiabá, Brazil, 2013.

[18] G.K. Vianna and S.M.S. Cruz, "Redes neurais artificiais aplicadas ao monitoramento da requeima em tomateiros," *Anais do X Encontro Nacional de Inteligência Artificial e Computacional (ENIAC)*, Fortaleza, Brazil, 2013.

[19] D. Nunes, C. Werly, G.K. Vianna, and S.M.S. Cruz. "Early Discovery of Tomato Foliage Diseases Based on Data Provenance and Pattern Recognition," *5th International Provenance and Annotation Workshop (IPAW)*. Cologne, Germany, 2014.

[20] J.C.A. Barbedo, "Digital image processing techniques for detecting, quantifying and classifying plant diseases," *SpringerPlus*, 2:660, 2013.

[21] A. Vibhute and S.K. Bodhe, "Applications of image processing in agriculture: a survey," *International Journal of Computer Applications*, vol. 52, n.2, pp.:34-40, 2012.

[22] I.M. Scotford and P.C.H. Miller, "Applications of spectral reflectance techniques in Northern European cereal production: a review," *Biosyst. Eng.*, vol. 90, n.3, pp.:235–250, 2005.

[23] C.H. Bock, G.H. Poole, P.E. Parker, and T.R. Gottwald, "Plant disease severity estimated visually, by digital photography and image analysis, and by hyperspectral imaging," *Critical Reviews in Plant Sciences*, vol. 29, n. 1-3, pp.:59–107, 2010.

[24] UCIPM – Integrated Pest Management Program of California University, Retrieved from: http://www.ipm.ucdavis.edu/DISEASE/DATABASE/potatolateblight.html, in June, 2016.

[25] R.A. Hyre, "Progress in forecasting late blight of potato and tomato". *Plant Disease Reporter*, Illinois, vol. 38, n.4, pp.: 245-253, 1954.

[26] INMET – Instituto Nacional de Meteorologia, Retrieved from: http://www.inmet.gov.br/portal/, in June 5th, 2016.

[27] T.N.H. Rebouças, et al. "Potencialidade de Fungicida e Agente Biológico no Controle da Requeima do Tomateiro", *Horticultura Brasileira*, vol.32(01), 2014.